Feasibility study for active debris removal mission

Project in SD2900 Fundamentals of Spaceflight, 2024

Team 2 - Ali Ghasemi, Anna Testani, Cassandra Oskarsson, Josephine Gurman, Kinane Obeidine

***Abstract*—ADR (Active Debris Removal) missions became crucial after the increase in space launches and the resulting congestion of Earth's orbit. It is essential not only to limit the production of further debris during new launches but also to implement re-entry plans for obsolete satellites, in order to mitigate the risk of collision, which is becoming the primary debris source. This paper aims to evaluate an ADR strategy from different perspectives: sustainability and feasibility both in terms of costs and technology readiness level (TRL). Results of this study indicate that ion propulsion systems are best for completing these types of missions along with the Electrodynamic Tether grabbing system. Moreover, one single satellite is not enough to meet all the duration and feasibility requirements and the costs associated with such a mission remain high.**

I. Introduction

This report is written as a part of a project in the course SD2900 Fundamentals of Spaceflight and contains a theoretical approach to ADR from Low Earth Orbit (LEO).

A. Background and motivation for the study

One significant consequence of launching rockets and satellites into space is the orbital debris left behind. The population of orbital debris is continuously growing, particularly in the region around lower LEO. The amount of debris in LEO has reached a level where, even without any future launches, the debris population will continue to increase [1]. As a result, it is essential to study strategies for removing orbital debris in LEO.

The goal is to conduct a feasibility study on a system, that can lower at least 10 rocket stages from their current orbits, in LEO, into a lower orbit with a maximum remaining orbital lifetime of 25 years. The project also aims to determine the time required to remove the debris, with a target time-frame of no more than one year. In addition to this, the study will also cover an evaluation of the project based on TRL.

B. Active Debris Removal state of art

No single capturing method is universally applicable to all types of debris in LEO. Based on [2], it is suggested to focus on tailored solutions for different types of debris. In terms of their characteristics, the methods are divided into two main categories: contact and contactless capturing methods.

Advantages and drawbacks exist for all options. After evaluating the average physical characteristics of the selected debris and considering the Δv cost, the Electrodynamic Tether (EDT) method is chosen from a comparison of five different methods: tether-based, laser-based, ion-beam shepherd-based, sail-based, and satellite-based. Three optimum capturing methods were identified and bar graph comparison (fig. 1) indicates that the tether-based method is the most suitable choice.

Some of the reasons that are taken into account for the selection of the tether-based capturing method are listed below:

- no external power requirement [3]
- effective in LEO [3]
- handling of moderate mass objects [2]
- flexibility and efficiency [3]

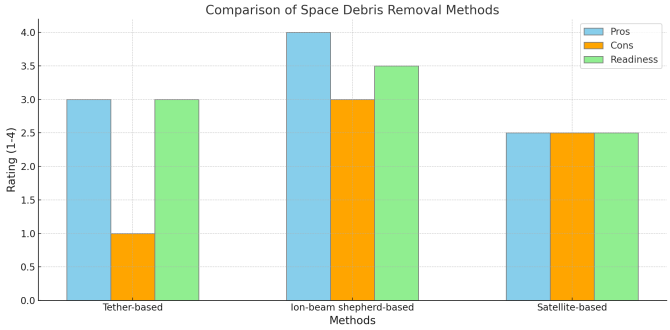

Fig. 1. Comparison of Top Three Space Debris Removal Methods for Rocket Debris

While there are four main types of tether-based approaches (see tab. IX), the EDT method emerges as the most effective for capturing rocket debris for the following reasons:

- suitable for debris in LEO [3]
- handling of moderate masses [2]
- no need for additional power [3].

C. General assumptions and limitations

The calculations in this report are based on various limitations and assumptions.

- Debris: because of low eccentricities, circular orbits with $r = a_{orbit}$ are assumed for the debris. Furthermore, due to unavailable data regarding debris dimensions, assumptions were made for the mass and cross-sectional area.
- Launch: the atmospheric density is assumed to be exponential till $150\,km$ and zero afterwards. Besides, Earth's rotation is not taken into account at the moment of launching. It is also assumed that the thrust vector and

the velocity vector have the same direction. Finally, lift is not considered.
- In-space maneuvers: two-body system equations are used and other effects on orbits are neglected (e.g. Earth's oblateness). The most conservative position is assumed to determine the rendezvous time.

D. Mission Outline

The proposed approach for completing the mission, while adhering to the requirements of a one-year timeline for the entire mission and a maximum decay time of 25 years, involves the launch of ten distinct satellites using the Falcon 9 rocket from SpaceX. Each satellite is equipped with an Ion Propulsion System (NEXT) and an EDT for debris capture. Following the launch, each satellite is tasked with intercepting a specific piece of debris, capturing it, and subsequently lowering its orbit to ensure decay within 25 years. The disposal orbits are selected to be at the same altitudes and to align with the initial orbital plane of each piece of debris to minimize Δv and Δt costs associated with plane changes.

II. Method – Debris

According to the project objectives, rocket bodies are considered for ADR. To find suitable debris, a database for satellites is searched [4]. For the selection of debris, it is important to minimize both the necessary right ascension of the ascending node (RAAN, Ω) and inclination (i) changes to keep the Δv in a feasible range. Thus, small $\Delta\Omega$ and small Δi are used for the data wrangling. For this, a higher priority is put onto low $\Delta\Omega$, as early calculations found RAAN changes to be especially expensive in terms of Δv. Also, the debris has to be found in LEO, which corresponds to a maximum altitude of $2000\,km$ above the Earth's surface. To decrease the needed Δv for in-plane maneuvers, the maximum altitude for the debris orbit should be as close to the graveyard orbit ($H_0 = 270\,km$, see IV-B) as possible.
The satellites are deployed on a parking orbit at altitude H_{park}, inclination i_{park}, and RAAN Ω_{park}. These were computed as the average values between all the selected debris:

$$\begin{cases} H_{park} = 740.49\,km \\ i_{park} = 91.39^\circ \\ \Omega_{park} = 269.48^\circ \end{cases} \tag{1}$$

III. Method – Launching

A. Launching vehicle

The rocket used for this mission is Falcon 9 which is a two-stage reusable rocket. Moreover, Falcon 9 rocket fits the mission requirements: it can deliver up to 20 tons of payload into LEO. In comparison with Ariane 5 and SLS, Falcon 9 shows better aspects as it is possible to recover its first stage and is cheaper [5]. The specifications according to [6] [7] can be found in tab. I.

TABLE I
Falcon 9 characteristics

	ISP (s)	Thrust (kN)	Burn time (s)	Dry mass ($tons$)	Propellant mass ($tons$)
First stage	282 (sea level)	7686	162	25.60	395.70
Second stage	346 (vacuum)	981	397	3.90	92.67

Both stages use nearly the same engine Merlin-1D++ – only the jet nozzle differs, having a thrust of $845\,kN$ at sea level and $981\,kN$ in vacuum. The number of engines differs for each stage, nine for the first and one for the second.

Falcon 9's nose has a diameter $D = 5\,m$, which leads to the reference area $A = 19.3\,m^2$. Its geometric shape guarantees a drag coefficient close to $C_d = 0.5$. Moreover, the propellant mass necessary for the first stage recovery is estimated at 20% of its total fuel capacity ($79.14\,tons$) in order to land on a sea platform.

B. Launching site

The chosen launch vehicle, Falcon 9, adheres to U.S. standards, which indicates that the launch site must be located within the United States. Furthermore, the parking orbit, i.e. the target orbit that the rocket aims to reach, plays a crucial role in determining the appropriate launch site. All calculations related to the launch site and launch window are based on spherical triangular geometry as shown in fig. 2.

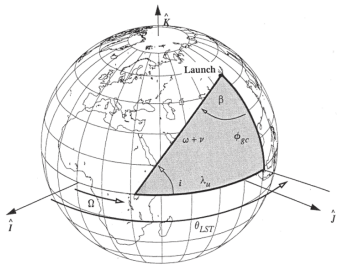

Fig. 2. Parameters for calculations of the launch site and launch window [8]

The equation used to determine the launch site is as follows:

$$cos(i_{park}) = cos(\phi_{cg})sin(\beta) \tag{2}$$

Where, β corresponds to the azimuth range for the launch site, ϕ_{cg} represents the latitude of the launch site, and i_{park} represents the inclination for the parking orbit, as shown in fig. 2. A table with values for the azimuth range and latitude of different launch sites can be found in [8]. For each U.S launch site, the corresponding range of inclinations is calculated, using eq. 2. However, it is important to note that the azimuth values provided by [8] are measured relative to due north, which means that it is needed to subtract 180° from the values of β when doing the calculations, i.e. $\beta_{south} = \beta_{north} - 180^\circ$, so that the values are measured relative to due south [9]. Since

the desired parking orbit's inclination is known (see eq. 1), the appropriate launch site can be selected accordingly.

The next step is to calculate the specific values of azimuth for the given inclination. For this, eq. 2 is rewritten so that β is calculated. Then it is necessary to add $180°$ to the calculated value to determine the azimuths for the prograde launch, i.e. $\beta_{prograde} = \beta + 180°$. The azimuth values for prograde launch, $\beta_{prograde}$, are then compared to the given azimuth range [8] measured relative to due south, β_{south}. This ensures that the comparison of the azimuth ranges is done accurately. The comparison indicates if $\beta_{prograde}$ is within the acceptable range for the azimuths for the chosen launch site. After this, the following equations are used to determine the launch window in local sidereal time:

$$\begin{cases} cos(\lambda_u) = \frac{cos(\beta)}{sin(i)} \\ \theta_{LST,1} = \Omega_{park} + \lambda_u \\ \theta_{LST,2} = \Omega_{park} + (180 - \lambda_u) \end{cases} \tag{3}$$

Where λ_u represents the angle between the node and the local longitude, Ω_{park} represents the RAAN for the parking orbit, and θ_{LST} corresponds to the launch window, also shown in fig. 2. The calculated azimuth, β, which is within the given azimuth range for the site, is used to calculate the λ_u in accordance to the system of equations 3. With the given RAAN for the parking orbit and the calculated value for λ_u, two possible launch windows, θ_{LST}, can be found as in eq. 3.

C. Launching trajectory

The launching of Falcon 9 must be made in order to put in orbit 10 satellites (one for each debris) at the altitude $H_{park} = 740.49\ km$. The speed to be reached is $V_{park} = \sqrt{\frac{\mu}{R_{earth}+H_{park}}} = 7.49\ km/s$ in order to be in a circular orbit at the right altitude.

In order to simulate the rocket's ascent phase, numerous assumptions are made. First, the rotation of the Earth is not considered when the rocket is launched, therefore the rocket does not have any horizontal velocity initially. Moreover, it is assumed that the rocket is equipped with a control system that forces the angle between velocity and thrust to be zero throughout the launch. Furthermore, the lift is not considered as the rocket's shape is symmetrical. Besides, density as a function of altitude is modeled as follows:

$$\begin{cases} \rho = \rho_0 e^{-\frac{z}{h}}, & z \leq 150\,km \\ \rho = 0, & z > 150\,km \end{cases} \tag{4}$$

where h is the scale height assumed to be constantly equal to $8.43\ km$. Due to minimal density for $z > 150\,km$, with $\rho(z = 150\,km) \simeq 10^{-9}\ kg/m^3$, it is assumed to zero.

With all these assumptions made and according to [10] the equations governing the rocket's motion are as follows:

$$\begin{cases} \dot{X} = V cos(\gamma) \\ \dot{H} = V sin(\gamma) \\ \dot{\gamma} = -\frac{1}{V}(g - \frac{V^2}{R_{earth}+H})cos(\gamma) \\ \dot{V} = \frac{T}{m} - \frac{D}{m} - gsin(\gamma) \\ \dot{m} = -m_{flow,i} \end{cases} \tag{5}$$

where $m_{flow,i}$ is the mass flow of the i^{th} stage ($i \in \{1, 2\}$). These equations take into account the curvature of the Earth. Drag is calculated through the formula $D = \frac{1}{2} C_d \rho A V^2$. This system of differential equations is solved numerically through Matlab® by using the function `ode45` with the following scheme

$$\begin{cases} \dot{u} = f(t, u) \\ u = (X, H, \gamma, V, m) \\ u(t = 0) = u_0 \end{cases} \tag{6}$$

For each variable X, H, γ, V and m, initial conditions are set in vector u_0. The launching is divided into 4 different phases, each one taking place over the time interval $[t_i, t_{i+1}]$:

1 – Vertical take-off $[0, t_1]$**:** the flight path angle is $\frac{\pi}{2}$, thrust is fully given by the first stage. For this initial phase, the initial conditions are $u_0 = (0, 0, \frac{\pi}{2}, 0, m_0)$.

2 – Start of gravity turn $[t_1, t_2]$**:** after a given time t_1 of vertical take-off, the rocket is tilted by γ_0. Therefore the flight path angle is $\frac{\pi}{2} - \gamma_0$, which leads to the beginning of the gravity turn. This phase ends when 80% of total propellant is consumed, then the first stage is released. The initial conditions are $u(t = t_1) = (X(t_1), H(t_1), \frac{\pi}{2} - \gamma_0, V(t_1), m(t_1))$

3 – Ignition of second stage $[t_2, t_3]$**:** second stage is ignited and gravity turn continues till the beginning of the next phase. The initial conditions for this phase are $u(t = t_2) = (X(t_2), H(t_2), \gamma(t_2), V(t_2), m(t_2) - m_{s1,dry})$

4 – Control of the flight path angle $[t_3, t_4]$**:** this occurs during the second stage phase at time t_3 and can last till the second stage burnout (but not necessarily). In this phase, the flight path angle is not a variable anymore and thus u becomes (X, H, V, m). Therefore, the flight path angle is controlled through a tangent steering law which is as follows:

$$\gamma(t) = \arctan\left(\tan(\gamma(t_3))\left(1 - \frac{t - t_3}{\Delta t_{ctrl}}\right)\right) \tag{7}$$

where $\Delta t_{ctrl} = t_4 - t_3$ is the total duration of the phase. At the end of this phase, the second stage's flight path angle is forced to zero and the stage is released with potentially some propellant left inside: in fact, the satellite is released at the exact moment when speed, altitude, and flight path angle values reach the boundary conditions which are related to the parking orbit. The initial conditions for this phase are $u(t = t_3) = (X(t_3), H(t_3), V(t_3), m(t_3))$.

With this description, one can highlight the following parameters influencing the altitude and speed that are reached at the end of the launching: tilt angle γ_0, vertical take-off time t_1, the time t_3 at which the control of flight path angle begins and its duration Δt_{ctrl}.

In order to adjust these parameters so that the circular orbit at altitude H_{park} is reached with the right speed V_{park} and flight path angle $0°$, the following method is adopted:

1) t_1 and γ_0 are manually adjusted
2) Δt_{ctrl} and t_3 are numerically adjusted by minimizing a cost function

$$\varphi : (t_3, \Delta t_{ctrl}) \longmapsto (V_f - V_{park})^2 + (H_f - H_{park})^2 \quad (8)$$

where V_f and H_f are the velocity and altitude of the satellite at the end of the 4^{th} phase that is obtained after the numerical resolution of the system of differential equations. The minimization is done by having recourse to the Matlab® function `fminsearch`.

For the first stage's recovery simulation, only the ballistic phase is simulated, without taking into account the rotation that needs to be made so that the stage lands correctly. Therefore, this descent phase starts after phase 2 and the system of equations 5 still stands with $T = 0$ for simplicity. Regarding the second stage, it is brought to the 25-years decay orbit ($H_0 = 270\,km$) through a Hohmann transfer.

IV. Method – Satellite

A. Satellite design

As mentioned in the ADR survey referenced in the introduction, the selected grabbing method is EDT.
For this ADR project, the NASA Evolutionary Xenon Thruster (NEXT) Ion Propulsion System is selected as the primary propulsion mechanism. Concerning the propulsion system, NEXT offers a high specific impulse of $I_{sp} \approx 4\,190\,s$, significantly surpassing traditional chemical propulsion systems and other electric propulsion options. This high I_{sp} translates to efficient propellant utilization, enabling the spacecraft to achieve the substantial Δv necessary for rendezvous with multiple debris targets while minimizing propellant mass. Moreover, NEXT has demonstrated remarkable durability and reliability through extensive testing. According to Patterson et al., [11], NEXT completed a continuous-duration test of over $50\,000\,h$ and processed more than $900\,kg$ of xenon propellant without significant degradation in performance. This longevity is essential for our mission, which requires sustained operation over extended periods to maneuver between debris objects in varying orbits. NEXT also provides a higher thrust-to-power ratio compared to previous ion propulsion systems, delivering up to $236\,mN$ of thrust at a power input of $6.9\,kW$ [12].

B. Orbit decay lifetime

To determine an orbit that meets the requirement of a 25-year decay time, the ballistic coefficient, which depends on the drag coefficient (C_d), debris' area (A), and mass (m), needs to be calculated (eq. 9). The behavior of altitude with time [10] can be approximated with eq. 10, while the decay time is calculated with eq. 11.

$$B^* = \frac{C_d A}{m} \quad (9)$$

$$H(t) = h\,ln\left[e^{\frac{H_0}{h}} - \frac{\sqrt{\mu R_e} B^* \rho_0}{h} t\right] \quad (10)$$

$$t_d = \frac{h}{\sqrt{\mu R_e} B^* \rho_0}\left(e^{\frac{H_0}{h}} - 1\right) \quad (11)$$

The mass considered is the sum of debris and satellite masses: $m = 85\,kg + 180\,kg = 265\,kg$. Assuming $C_d = 2.2$ and $A = 1\,m^2$ for each debris, the trend of altitude over time is plotted for different altitudes in the range $[260\,km; 290\,km]$, see fig. 3. Since it is most accurate to use the scale height at the lower altitude [13], the height scale and density are assumed: $h_{@250km} = 44.924\ km$ and $\rho_{0,@500km} = 6.073 \cdot 10^{-11}\ kg/m^3$.

To keep costs down, the $270\ km$ orbit is chosen since it is the highest one to fit the requirement. It would be more expensive to bring the debris to a lower orbit, even if it took a shorter period to decay. Thus, the objective is to bring the debris on a circular orbit with altitude $H_0 = 270\ km$. The calculations show that this will decay in $22.79\ years$.

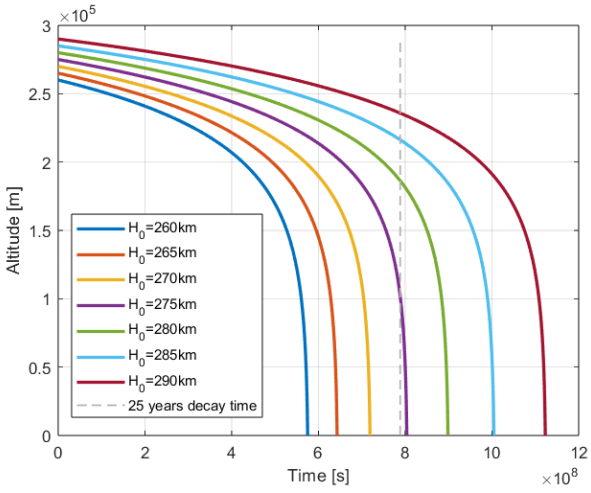

Fig. 3. Trend of altitude over time

C. In-space maneuvers

To simplify the calculations, all orbits are assumed to be circular, as their eccentricities are nearly zero. Consequently, the arguments of perigee are set to zero, and the orbital radii are taken as equal to the semi-major axes. These values are chosen with the aim of lowering Δv and time costs.
Once all the satellites are on this parking orbit, each one will follow a specific thrust scheme in order to reach the respective debris' orbit, grab it, and then come back to the disposal orbit:

- Change of semi-major axis: from r_{park} to r_{db}, radius of debris' orbit. This is accomplished with a spiral maneuver:

$$\Delta v_1 = \left|\sqrt{\frac{\mu}{r_{park}}} - \sqrt{\frac{\mu}{r_{db}}}\right| \quad (12)$$

  This maneuver is executed prior to the plane change only if $r_{db} > r_{park}$, otherwise, it is performed after the inclination and RAAN changes. This is because the Δv costs for these two maneuvers are proportional to the orbital velocity, making it more efficient to conduct them

in a higher, and thus slower orbit. Consequently, for eq. 13 and 14:

$$\begin{cases} r = r_{db} & \text{if } \; r_{db} > r_{park} \\ r = r_{park} & \text{if } \; r_{db} < r_{park} \end{cases}$$

- Change of inclination: from i_{park} to i_{db}, inclination of debris' orbit.

$$\Delta v_2 = \sqrt{\frac{\mu}{r}} \sqrt{2 - 2\cos\left(\frac{\pi}{2}(i_{db} - i_{park})\right)} \tag{13}$$

- Change of RAAN: from Ω_{park} to Ω_{db}, RAAN of debris' orbit.

$$\Delta v_3 = \frac{\pi}{2}\sqrt{\frac{\mu}{r}}\,|\Omega_{db} - \Omega_{park}|\sin i_{db} \tag{14}$$

- Change of semi-major axis: after rendezvous (see sec. IV-D), this last maneuver is performed to arrive at the disposal orbit, which has the same inclination and RAAN of the debris' orbit and altitude H_0 ($r_0 = R_e + H_0$).

$$\Delta v_4 = \sqrt{\frac{\mu}{r_0}} - \sqrt{\frac{\mu}{r_{db}}} \tag{15}$$

Assuming a constant acceleration $A = 0.1 mm/s^2$, time is computed for every maneuver as:

$$\Delta t_i = \frac{\Delta v_i}{A} \tag{16}$$

D. Rendezvous

To estimate the time and Δv costs for rendezvous, it is assumed, in the worst-case scenario that the satellite is half an orbit behind the debris (or ahead). To reach the debris, the satellite must transition to a lower elliptical orbit by applying thrust at any point along the circular debris orbit, in the direction opposite to its motion, thereby lowering its perigee. The new semi-major axis is selected such that, while the debris completes 24.5 orbits, the satellite completes 25 (fig. 4). In this way, the new orbit will be only slightly smaller than that of the debris, minimizing the Δv cost.

$$25\,P_s = 24.5\,P_{db} \;\rightarrow\; 25 \cdot 2\,\pi\sqrt{\frac{a_s^3}{\mu}} = 24.5 \cdot 2\,\pi\sqrt{\frac{a_{db}^3}{\mu}} \tag{17}$$

$$a_s = a_{db}\sqrt[3]{\frac{24.5^2}{25^2}} \tag{18}$$

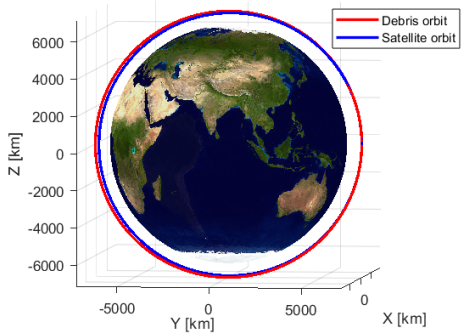

Fig. 4. Example of rendezvous

The Δv is computed as the difference between the velocity on the circular debris orbit and the velocity at the apogee of the new orbit, multiplied by two (see eq. 19). This accounts for the fact that the satellite must apply a second thrust at the end of the maneuver to match the debris' speed.

$$\Delta v_{rv} = 2 \cdot \left(\sqrt{\frac{\mu}{a_{db}}} - \sqrt{\frac{2\mu}{a_{db}} - \frac{\mu}{a_s}}\right) \tag{19}$$

Finally, the time required for each rendezvous is $\Delta t_{rv} = 24.5\,P_{db}$.

V. Method – Cost Analysis and Sustainability

According to [14], the cost analysis can be conducted by dividing it into several different parts. Using the cost estimation model from [14], the development costs can be calculated with:

$$C_{\text{development}} = C_0 \cdot \left(\frac{M}{M_0}\right)^x \tag{20}$$

Operational costs are estimated with

$$C_{\text{ops}} = C_{\text{ops,0}} \cdot T^{\beta} \tag{21}$$

where $C_{\text{ops,0}}$ is the base operation cost, T is the mission time and β the cost scaling exponent. [14]

Accounting for potential cost overruns of about 45% as suggested by [15], the total cost estimation is adjusted in this manner: $C_{\text{total,adjusted}} = 1.45 \cdot C_{\text{total}}$.

To understand the environmental impact of rocket launches on the global environment, the total energy needed per launch is compared with a long-distance flight. For an estimated energy consumption for a long-duration flight, the equation from [16] is used (see eq.22).

$$E_{flight} = t_{\text{flight}} \cdot \left(\frac{1}{2} \cdot c_d \rho A_p v^3 + \frac{1}{2} \cdot \frac{(mg)^2}{\rho v A_s}\right) \tag{22}$$

Meanwhile for the launch, the energy consumption is calculated as follows:

$$E_{rocket} = U \cdot V \tag{23}$$

where U is the energy density of the propellant (LOX / RP-1) and V the volume of propellant contained in the rocket. To complete the study regarding the sustainability aspect, one must discuss the propellant impact on the environment and if the quantity of propellant used during the launch is optimized.

VI. Results

A. Debris

Fitting the requirements, ten pieces of debris can be found within $\Delta\Omega = 9.00°$, $\Delta i = 17.59°$ and $h_{max} = 1017\,km$. The orbital elements for the debris can be found in tab. II. In fig. 5, the corresponding orbits are shown.

TABLE II
ORBITAL PARAMETERS OF SELECTED SPACE DEBRIS

Official Name	Satellite Number	Apogee $[km]$	Perigee $[km]$	Inclin. $[°]$	RAAN $[°]$	Arg. of Per. $[°]$
SL-3 R/B	06393	7 356	7 272	81.25	267.33	14.42
SL-14 R/B	16882	6 986	6 962	82.52	265.39	289.32
ATLAS 28E R/B	20563	7 038	6 957	89.85	267.46	273.21
SL-14 R/B	21398	6 999	6 967	82.52	272.19	110.20
TAURUS R/B	25490	7 033	7 014	85.06	266.91	210.52
PSLV R/B	25759	7 085	7 046	98.66	271.52	20.46
MINOTAUR R/B	28637	7 173	7 155	98.75	268.42	271.76
CZ-11 R/B	43161	7 388	6 865	98.21	274.39	171.52
CZ-2D R/B	54030	7 078	7 050	98.20	270.73	61.24
CZ-6A R/B	54236	7 200	7 138	98.84	270.49	320.84

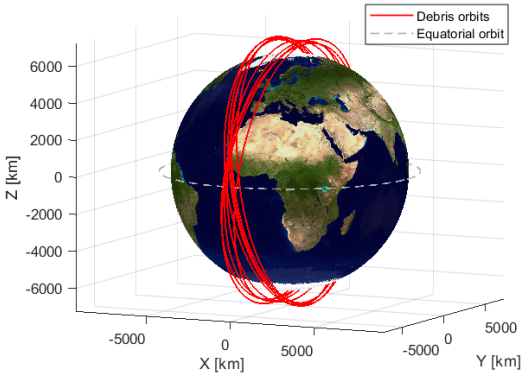

Fig. 5. Debris Orbits around Earth

B. Launch site

The results of the ranges for inclinations corresponding to the launching sites in the U.S., calculated with eq. 2, are shown in tab. III.

TABLE III
RANGE OF INCLINATIONS FOR LAUNCH SITES IN THE U.S

U.S Launch site	i_{min} $[°]$	i_{max} $[°]$
Vandenberg	72.84	116.64
Cape Kennedy	121.93	144.57
Wallops	113.25	130.30

Since the given inclination for the desired parking orbit is $i_{park} = 91.39°$, the Vandenberg launching site is chosen, which has a latitude of $\phi_{cg} = 34.6°$ [8].

The results for the azimuths for the given inclination, i_{park}, and launch site latitude ϕ_{cg} are presented in tab. IV.

TABLE IV
SPECIFIC AZIMUTHS,β,FOR GIVEN INCLINATION

β_1 $[°]$	$\beta_{1prograde}$ $[°]$	β_2 $[°]$	$\beta_{2prograde}$ $[°]$
-1.68	178.32	181.68	361.68

The range of the azimuth for Vandenberg provided in [8] is $\beta_{north} = [147, 201]$ relative to due north and therefore $\beta_{south} = [-33, 21] = [327, 21]$ relative to due south. By comparing the values for $\beta_{prograde}$, shown in tab. IV, and the range β_{south}, it can be concluded that only $\beta_{2prograde} = 361.68° = (361.68 - 360)° = 1.68°$ is within the range, and therefore it is the only acceptable launch azimuth.

By using $\beta_2 = 181.68°$, for calculating eq. 3, the result is $\lambda_u = 179.04°$. Combining $\lambda_u = 179.04°$ and the given RAAN, $\Omega_{park} = 269.48°$, in accordance to eq. 3, results in two launch windows at $\theta_{LST1} = 88.53°$ and $\theta_{LST2} = 270.44°$.

C. Launch trajectory

As mentioned in III-C, one must adjust the parameters so that the satellite is put into orbit at the right altitude with the right speed and flight path angle ($H_{park} = 740.49\ km$, $V_{park} = 7.49\ km/s$ and $\gamma_{park} = 0°$).

Tab. V sums up the values that were taken for all parameters:

TABLE V
ADJUSTED VALUES FOR LAUNCHING PARAMETERS

γ_0 $(°)$	1 (manually adjusted)
t_1 (s)	30.00 (manually adjusted)
t_3 (s)	290.08 (numerically adjusted)
Δt_{ctrl} (s)	136.94 (numerically adjusted)

With these values, fig. 6 contains the results regarding the evolution of altitude, velocity and flight path angle. Phase 5 is plotted to show that after phase 4, the satellite's orbit is indeed circular as the altitude and speed are constant in time. First stage's recovery is also observed.

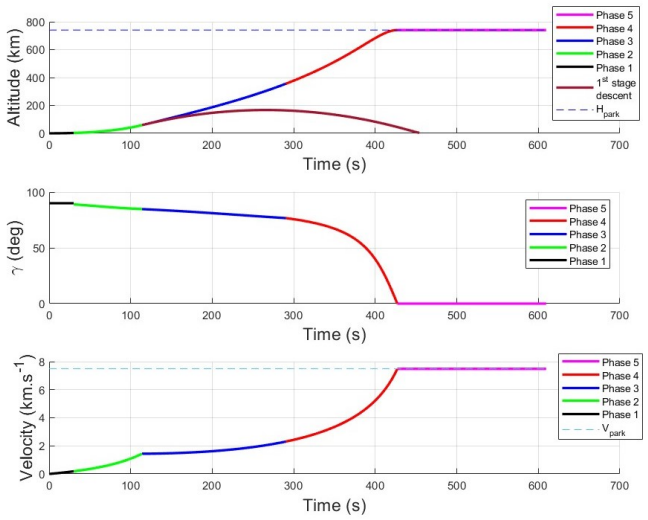

Fig. 6. Evolution of Velocity, Altitude and Flight Path Angle

Regarding the second stage, the quantity of propellant left inside at the end of phase 4 is $2.183\ tons$, the total mass is therefore $6.083\ tons$. For a Hohmann transfer, the Δv needed to go from the parking orbit to the decay orbit is

$$\Delta v = \Delta v_1 + \Delta v_2 \tag{24}$$

where

$$\Delta v_1 = \sqrt{\frac{2\mu}{r_0} - \frac{2\mu}{r_0 + r_{park}}} - \sqrt{\frac{\mu}{r_0}} = 130.21\ m/s \quad (25)$$

and

$$\Delta v_2 = \sqrt{\frac{\mu}{r_{park}}} - \sqrt{\frac{2\mu}{r_{park}} - \frac{2\mu}{r_0 + r_{park}}} = 132.48 m/s \quad (26)$$

. Through Tsiolkovsky equation, an estimation of the propellant mass needed for the transfer is obtained, which is $453.1\,kg$. Therefore, there is enough propellant left. The transfer is observed in fig. 7.

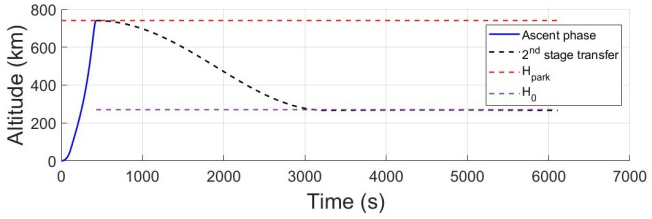

Fig. 7. Evolution of altitude for second stage

D. In-space maneuvers

In tab. VI below, results for the in-space maneuvers Δv are shown.

TABLE VI
Δv COST-RESULTS

Sat. $N°$	Δv_1 [km/s]	Δv_2 [km/s]	Δv_3 [km/s]	Δv_4 [km/s]	Δv_{rv} [km/s]	Δv_{tot} [km/s]
06393	0.0633	1.8157	0.8326	0.1974	0.1027	3.0117
16882	0.0391	1.2960	0.5254	0.2216	0.1024	2.1844
20563	0.0738	2.0528	0.4320	0.3344	0.1009	2.9939
21398	0.0515	0.3154	0.4147	0.2092	0.1026	1.0933
25490	0.0620	1.4957	0.2144	0.3226	0.1010	2.1957
25759	0.0670	1.5132	0.2017	0.3277	0.1010	2.2106
28637	0.0141	1.3972	0.2532	0.2466	0.1021	2.0131
43161	0.0127	1.4898	0.4134	0.2479	0.1020	2.2659
54030	0.0571	1.8154	0.5507	0.2036	0.1026	2.7294
54236	0.0296	1.3935	0.9924	0.2903	0.1015	2.8073

The results for time are presented in tab. VII.

TABLE VII
Δt COST-RESULTS

Sat. $N°$	Δt_1 [days]	Δt_2 [days]	Δt_3 [days]	Δt_4 [days]	Δt_{rv} [days]	Δt_{tot} [days]
06393	7.3	210.2	96.4	22.8	1.7	338.3
16882	4.5	150.0	60.8	25.6	1.7	242.6
20563	8.5	237.6	50.0	38.7	1.7	336.6
21398	6.0	36.5	50.0	24.2	1.7	116.3
25490	7.2	173.1	24.8	37.3	1.7	244.2
25759	7.8	175.2	23.3	37.9	1.7	245.9
28637	1.6	161.7	29.3	28.5	1.7	222.9
43161	1.5	172.4	47.8	28.7	1.7	252.1
54030	6.6	210.1	63.7	23.6	1.7	305.7
54236	3.4	161.3	114.9	33.6	1.7	314.9

The total mission duration is the longest Δt among those presented: $\Delta t_{tot} = 338.3\ days$.

E. Cost analysis and sustainability

To determine the cost of this mission, the mass of the required systems has to be estimated.
First, the necessary propellant for the satellite is calculated with the Tsiolkovsky rocket equation utilizing the desired Δv to determine one satellite's total mass, where $I_{\text{sp, NEXT}} = 4\,190s$ [17], [18]. With this, the propellant mass can be considered as approximately 7.85% of the dry mass of the satellite.

Tab. VIII summarizes the mass distribution among the satellite's subsystems based on typical values from similar missions [19].

TABLE VIII
SATELLITE MASS BREAKDOWN

Subsystem	**Mass (kg)**
Propulsion System (dry)	13
Propellant (Xenon)	13.47
Electrodynamic Tether System	9
Power System	49.5
Structure and Mechanisms	60
Attitude Determination and Control System (ADCS)	20
Communication System	10
Onboard Data Handling	5
Payload	5
Total Dry Mass	171.5
Total Wet Mass	184.97

The development costs can be estimated to \$77 million, where $C_0 = \$50$ million, $M = 1\,715kg$ is the total dry mass of ten satellites, $M_0 = 1\,000$ kg, and $x = 0.8$ (see eq. 20). The values for C_0 and M_0 are chosen as these are average values used for space missions. The typical range for X is $[0.6; 0.8]$, with 0.8 being chosen due to the higher complexity of the mission [14].

The launch cost for a Falcon 9 is approximately \$67 million. Since the total payload mass is within the Falcon 9's capacity (up to 22 800 kg to LEO), the cost remains at this rate [20].

The base operational costs for comparable missions in LEO are estimated to reach up to $C_{\text{ops},0} = \$10$ million annually, which can be chosen considering that ADR is an emerging field with limited historical data, which may lead to higher operational expenses due to its novelty and associated technological challenges. This corresponds to $C_{\text{ops}} = \$10$ million.

Adding up all of the mentioned cost factors, the estimated, total cost is $C_{\text{total}} = \$154$ million. Including the 45% margin, the total, adjusted cost can be estimated to \$223.3 million.

Furthermore, for the sustainability, using eq. 22 with the values suggested by [16], and an average long-distance flight duration of $12\,h$ [21], the resulting total energy consumption of a long-duration flight is $E_{\text{flight}} = 1.574 \cdot 10^{12}$ J. For the rocket, by using eq. 23, with an energy density of $43 \cdot 10^6\,J/kg$ according to [22] and a total of $488.37\,tons$ of fuel for both stages, the resulting overall energy consumption for a rocket launch with Falcon 9 is $E_{\text{rocket}} = 2.1 \cdot 10^{13}\ J$.

Moreover, as mentioned in the launching results, there is $1\,729.9\ kg$ of propellant left after its transfer to the decay

orbit, which must be discussed from the sustainability point of view.

VII. Discussions

A. Debris

Numerous pieces of debris could have been suitable targets for this work. However, the constraints imposed by the fixed type of debris, and the limitations associated with the Δv regarding RAAN and inclination, restrict the viable combinations of accumulating ten debris pieces. With increased time and resources, it is likely that more suitable and cost-effective debris targets (in terms of Δv) could have been identified for this mission.

B. Launching

The Falcon 9 launch vehicle is selected because it is reusable, which means that it has the possibility to reuse its first stage instead of throwing it into space. This aligns with the mission's objective of space debris collection, as only the second stage is thrown into space while the first stage is recovered.

Given the use of the Falcon 9, the launch site, as previously mentioned, has to be located in the United States. However, if a launch vehicle with European standards had been used instead, the launch site could possibly have been located closer to the equator, for example, the Kourou launch site [8]. A launch site closer to the equator would have offered a more optimal and efficient launch. Furthermore, a prograde launch means that the launch is done to the east. This is preferred since the rotation of the earth will minimize the amount of propellant required to reach the parking orbit [9]. For the resulting launch windows, one of the angles was initially $\theta_{LST} = 448.53°$. However, since this exceeds a full circle, $360°$ was subtracted, yielding a value of $\theta_{LST} = 88.53°$, as stated in the results for the launch site. This adjustment of the launch window angle is reasonable, since the condition $i > \phi_{cg}$ is true, which confirms the presence of two launch windows within each 24-hour period [23].

Regarding the launch trajectory, numerous aspects can be discussed. First of all, as seen in fig. 6 the flight path angle decreases quickly (from 80° to 0° in less than 140 seconds), therefore the assumption that the angle between the velocity vector and the thrust vector is zero might be questioned. Moreover, the drag coefficient is assumed to be 0.5 which is only an average value for a rocket as there is no accurate data for the Falcon 9 rocket. Finally, the atmosphere model could be reviewed as density is assumed to be zero after $150\,km$ to gain accuracy. Nonetheless, when the $150\,km$ limit is changed to $50\,km$, the value for the numerically adjusted parameters t_3 and Δt_{ctrl} vary by less than $0.4s$ for each – which is negligible.

C. Satellites

1) Grabbing method: The tether-based EDT method is chosen for its advantages, however one must also discuss its drawbacks. Indeed, it has a slower process [24] and a risk of impact with other small debris in LEO.

2) Decay lifetime: Calculations for the orbit's decay lifetime are based on very strong assumptions, starting from the exponential atmospheric model. Both the base atmospheric density, ρ_0, and the scale height, h, can fluctuate significantly over short time scales, particularly during solar storms. Furthermore, these parameters vary with the phase of the 11-year solar cycle, introducing substantial inaccuracies in long-term orbital decay predictions [10].

To calculate orbit's decay lifetime it is necessary to estimate the debris drag coefficient. The latter varies depending on several factors such as its shape, orientation, and surface properties. However, a reasonable estimation can be provided based on existing studies. For most debris objects in LEO, the drag coefficient typically falls within the range of 2.0 to 2.5. This range accounts for the fact that space debris usually have an irregular shape and are subject to rarefied gas dynamics due to the low atmospheric density at those altitudes [25].

3) In-space maneuvers: Low-thrust propulsion is selected after evaluating the Δv requirements for high-thrust maneuvers. Indeed, using a Hohmann transfer and impulsive plane changes, the total cost is calculated as $\Delta v_{ht} = 38.5\,km/s$, which is beyond the capabilities of any currently available high-thrust propulsion systems. Additionally, the computed final-to-initial mass ratio, assuming $I_{sp} = 400s$, results in $\mu = 5 \cdot 10^{-5}$, a value that is clearly unfeasible.

Furthermore, calculations are performed to assess the feasibility of completing the entire mission with a single satellite. However, results indicated that the trajectories would require more than 400 days to complete. Consequently, it was decided to deploy ten separate satellites, each tasked with intercepting a different piece of debris.

From tab. VI, it can be noted that the highest Δv cost is primarily due to the inclination change. A change in RAAN would have been even more effective if the constraint on the allowable range had not been set so restrictive for the choice of debris. Finally, it can be observed that the rendezvous costs are minimal.

From tab. VII, it is clear that all thrust schemes satisfy the one-year duration requirement. Another notable detail is that the rendezvous time is approximately the same for each piece of debris, as they are all at similar altitudes.

4) Importance of satellites: One must keep in mind the importance of sending satellites. They are indeed essential for fostering a sustainable society through various critical applications. For example, in telecommunications, they enable global connectivity, especially in remote areas such as education, healthcare, and economic growth. Earth observation satellites monitor climate change, track deforestation, and aid in disaster management with GPS technology. They are also fundamental for national security by providing surveillance. Furthermore, satellites contribute to scientific advancements, offering data for space research and technologies that improve life on Earth. Therefore, satellite technology drives both sustainable development and global security.

D. Cost analysis

Cost estimation for space missions is often highly uncertain due to technical complexities and varying project requirements. The estimated costs should therefore be treated with considerable caution. However, even approximate estimates are essential for budgeting and decision-making, as they provide a baseline for resource allocation and feasibility assessments, guiding project stakeholders in the mission development process.

E. Sustainability

Ion thrusters use inert gases like xenon, resulting in minimal environmental impact both during operation and in terms of propellant handling. This aligns with increasing industry emphasis on sustainable space operations [26]. In contrast, chemical engines often use toxic propellants like hydrazine, posing environmental and safety risks during fuel processing and potential contamination upon release. Hybrid systems mitigate some environmental concerns by incorporating electric propulsion phases but still involve chemical propellants for certain maneuvers.

For the launch, as mentioned in the results, the initial quantity of propellant in the second stage is higher than necessary which has an environmental impact. Trajectory parameters must be adjusted in order to minimize the propellant left in the second stage which could be done by introducing a new cost function ψ as follows

$$\psi : (t_1, \gamma_0, t_3, \Delta t_{ctrl}) \rightarrow (V_f - V_{park})^2 + (H_f - H_{park})^2 + m_f^2 \quad (27)$$

where m_f is the mass of propellant. Moreover, the second stage is not reusable as it is to the decay orbit.

Generally, the environmental impact of a rocket launch, on a global scale, is related to greenhouse gas emissions and ozone layer depletion. Rocket launches emit large amounts of carbon dioxide and water vapor into the atmosphere, which contribute to global warming. Additionally, solid rocket propellants release chemicals that are harmful to the ozone layer [27], which is negative since the ozone layer protects Earth from harmful UV radiation. However, the environmental impact on the local area around the launch site mainly consists of air, water and soil pollution, high level of noise, and habitat disturbance. During launches, rockets produce exhaust gases containing toxic chemicals that can contaminate the air in the surrounding regions. These pollutants may also contaminate nearby soil and water bodies when debris or propellant lands in the oceans. Rocket launches generate extremely loud noise, which can disturb local wildlife and humans in the surrounding regions. Other elements that can disturb the wildlife habitat are the vibrations and the infrastructure required for launch sites [27]. Specific for the Vandenberg launch site is that the surrounding area is inhabited by a diverse range of wildlife including threatened and endangered species of animals [28]. Therefore, launching from this site is particularly negative in this aspect.

The results of the comparison between a long-duration flight and a rocket launch, shows that the rocket launch has an energy consumption that is ten times higher than a long-distance flight. However, since the number of long-duration flights that occur everyday is much higher than the number of rocket launches, this number can be seen as reasonable in the aspect of sustainability.

F. Technology Readiness Level

Since the chosen launch vehicle for the project, Falcon 9, has been used in successful missions multiple times [29], the technology can be rated as TRL 9 in accordance to [30].

The TRL for EDT methods can vary depending on specific applications, designs, and mission readiness. However, as of recent evaluations, these systems are typically considered to be at TRL 5. For EDT systems, this means that prototypes have been tested in conditions that simulate space or have undergone relevant experiments in orbit. [30]

NEXT is a well-established technology that has been demonstrated and used in various space missions. As of the latest evaluations, NEXT is generally considered to be at TRL 9.

VIII. Conclusions

In conclusion, the urgency of rapid response in space debris management necessitates selecting the most practical propulsion and grabbing systems to ensure mission efficiency. Relying on multiple smaller satellites instead of a single, large one reduces the risk of mission failure and simplifies technological and manufacturing processes, making the mission more robust and manageable. Additionally, focusing on debris with similar characteristics, particularly in terms of RAAN and inclination, can lead to significant cost savings, optimizing the mission's overall effectiveness and affordability. These strategies collectively contribute to a more feasible and sustainable approach to space debris mitigation.

Future efforts should address the high total cost of the mission by exploring more cost-efficient technologies and materials. Improving precision and control, especially for debris capture, can be achieved through autonomous systems utilizing computer vision, which would reduce dependency on manual operations from Earth. Investigating the use of rockets powered by green energy could significantly reduce the environmental impact of the mission. Additionally, building space stations dedicated to recycling debris could transform space waste into reusable materials, offering a sustainable alternative to burning debris in Earth's atmosphere. These advancements could lead to more efficient and environmentally friendly space missions.

IX. Division of work

The work was divided as follows.

Ali Ghasemi: Methods and Results for Satellite (design, cost analysis), Discussion for Satellite (propulsion and grabbing system discussion), Cost analysis, Sustainability, Conclusion.

Anna Testani: Methods and Results for Satellite (orbit decay lifetime, maneuvers), Discussion for Satellite (decay lifetime, maneuvers, TRL), Abstract, Mission outline.

Cassandra Oskarsson: Methods and Results for launch site, Discussions for Launching, Sustainability and TRL, Introduction.

Josephine Gurman: Methods and Results for debris and cost analysis, Discussions for Debris, Cost analysis and Sustainability, References, Introduction.

Kinane Obeidine: Methods and Results for launching vehicle and trajectory, Discussions for Launching and Sustainability.

REFERENCES

[1] J.-C. Liou, N. L. Johnson, and N. M. Hill, "Controlling the growth of future leo debris populations with active debris removal," *Acta Astronautica*, vol. 66, pp. 648–653, 2010.

[2] M. Shan, J. Guo, and E. Gill, "Review and comparison of active space debris capturing and removal methods," https://doi.org/10.1016/j.paerosci.2015.11.001, 2016, accessed: 2024-09-25.

[3] Y. Ohkawa, S. Kawamoto, T. Okumura, K. Iki, H. Okamoto, K. Inoue, T. Uchiyama, and D. Tsujita, "Review of kite – electrodynamic tether experiment on the h-ii transfer vehicle," 2020, accessed: 2024-09-25.

[4] N2YO.com, "N2yo satellite tracking," https://www.n2yo.com, 2024, accessed: 2024-09-26.

[5] "How much does it cost to launch a rocket? [by type size]," https://spaceimpulse.com/2023/08/16/how-much-does-it-cost-to-launch-a-rocket/, 2023, accessed: 2024-10-16.

[6] wevolver.com, "Falcon 9 v1.2 or full thrust - block 5," https://www.wevolver.com/specs/falcon-9-v12-or-full-thrust-block-5, 2024, accessed: 2024-09-21.

[7] spacex.com, "Falcon 9," https://www.spacex.com/vehicles/falcon-9/, 2024, accessed: 2024-09-21.

[8] M. Peet, "Spacecraft dynamics and control [powerpoint slides]," https://control.asu.edu/Classes/MAE462/462Lecture09.pdf, 202A.

[9] M.Peet, "Lecture 9: Bi-elliptics and out-of-plane maneuvers [youtube video]," https://youtu.be/aQr6zFRh2xI?si=VqHxjyhHzJMPW-3S, 2021.

[10] W. E. Wiesel, *Spaceflight Dynamics*. McGraw-Hill, 2010.

[11] D. A. Herman, "Nasa's evolutionary xenon thruster (next) project qualification propellant throughput milestone: Performance, erosion, and thruster service life prediction after 450 kg," https://ntrs.nasa.gov/citations/20110000521, 2010, accessed: 2024-09-25.

[12] N. G. R. Center, "Next-c ion propulsion system fact sheet," 2021, accessed: 2024-09-25.

[13] G. Tibert, "Reentry dynamics," Lecture slides, pp. 26–27, 2024, sD 2900 Fundamentals of SpaceflightCourse Name, KTH Stockholm, 26.08.2024. [Online]. Available: https://canvas.kth.se/courses/49442/files/folder/Lecture%20slides/Gunnar%20Tibert's%20lecture%20slides?preview=8179660

[14] J. R. Wertz and W. J. Larson, *Space Mission Analysis and Design*, 3rd ed. Microcosm Press and Kluwer Academic Publishers, 1999.

[15] S. Keller, P. Collopy, and P. Componation, "What is wrong with space system cost models? a survey and assessment of cost estimating approaches," *Acta Astronautica*, vol. 93, pp. 345–351, 2014.

[16] D. J. MacKay, *Sustainable Energy — without the hot air*, version 3.5.2 ed. UIT Cambridge, November 2008.

[17] A. Sengupta, J. R. Brophy, and J. E. Polk, "Status of the next ion engine 2000 hour wear test," in *42nd AIAA/ASME/SAE/ASEE Joint Propulsion Conference & Exhibit*, 2006.

[18] G. P. Sutton and O. Biblarz, *Rocket Propulsion Elements*, 8th ed. John Wiley & Sons, 2010.

[19] J. R. Wertz, D. F. Everett, and J. J. Puschell, *Space Mission Engineering: The New SMAD*. Microcosm Press, 2011.

[20] SpaceX. (2021) Smallsat rideshare program.

[21] Wikipedia contributors, "Flight length," 2024, accessed: 2024-10-01. [Online]. Available: https://en.wikipedia.org/wiki/Flight_length

[22] E. Gofman, "Energy of density of aviation fuel," https://hypertextbook.com/facts/2003/EvelynGofman.shtml, 2003.

[23] L. George, "Launch windows and time," https://oer.pressbooks.pub/lynnanegeorge/chapter/launch-windows-and-time/, accessed: 2024-09-28.

[24] C. P. Mark and S. Kamath, "Review of active space debris removal methods," https://doi.org/10.1016/j.spacepol.2018.12.005, 2019, accessed: 2024-09-25.

[25] D. A. Vallado and D. Finkleman, "A critical assessment of satellite drag and atmospheric density modeling," *Acta Astronautica*, vol. 95, pp. 141–165, 2014.

[26] Levchenko et al., "Space micropropulsion systems for Cubesats and small satellites: From proximate targets to furthermost frontiers," https://ui.adsabs.harvard.edu/abs/2018ApPRv...5a1104L, Mar. 2018.

[27] R. S. A. G. J. S. S. . D. A. Dallas, J.A., "The environmental impact of emissions from space launches: A comprehensive review," *Journal of Cleaner Production, Vol. 255*, 2020.

[28] R. Quijas, "Preserving nature, empowering launch," https://www.vandenberg.spaceforce.mil/News/Article-Display/Article/3786766/preserving-nature-empowering-launch/, 2024, accessed: 2024-10-01.

[29] Wikipedia contributors, "List of falcon 9 and falcon heavy launches," https://en.wikipedia.org/wiki/List_of_Falcon_9_and_Falcon_Heavy_launches, 2024, accessed: 2024-10-01.

[30] T. Sénéchal and O. Talon, "Use of lca for accompanying innovation processes all along the trl scale," 2016.

APPENDIX

TABLE IX
COMPARISON OF TETHER-BASED DEBRIS REMOVAL METHODS

Tether Method	**Description**	**Pros**	**Cons**
EDT	Involves a long, electrically conductive tether interacting with Earth's magnetic field to generate a drag force and remove debris	Effective for debris in low Earth orbit (LEO); can deorbit multiple pieces of debris over time	Very slow process and vulnerable to impacts from other debris
Tether-Nets	A tether connected to a net that captures targeted debris and pulls it into a deorbiting path	Can capture large, irregular-shaped debris, and adaptable to various sizes	Deployment can be tricky with a risk of tangling or missing the target
Harpoon Tethers	A tether system with a harpoon attached at the end to penetrate and capture debris	Suitable for debris with a solid structure; can capture debris at various orientations	Risk of creating additional debris if the harpoon misses or dislodges parts
Hybrid Tether Systems	Combines multiple tether techniques, such as nets, hooks, and harpoons, to capture and remove debris	More versatile and adaptable to different types of debris in various orbits	More complex and potentially challenging to implement